A comparison of measurements on electronic transport through molecules

Ilias Katsouras

Supervised by Dr. Bert de Boer

University of Groningen
Zernike Institute for Advanced Materials
Faculty of Mathematics and Natural Sciences

Groningen
June 2007

Abstract

A deceptively easy question in the field of molecular electronics: *"What is the conductance of a single molecule?"* has proved to be a rather difficult one to answer. The conductance of a molecule depends not only on the intrinsic properties of the molecule, but also on the electrode materials, the characteristics of the molecule-electrode contacts and the local environment of the molecule. This review provides an overview of the experimental techniques that are being used to measure the electron transport properties of molecules, discusses the advantages and drawbacks of these techniques and explores the critical parameters during such experiments.

Contents

1. Introduction

Gordon E. Moore, co-founder of Intel, observed in 1965 that the number of transistors on an integrated circuit for minimum component cost doubles every 24 months [1].

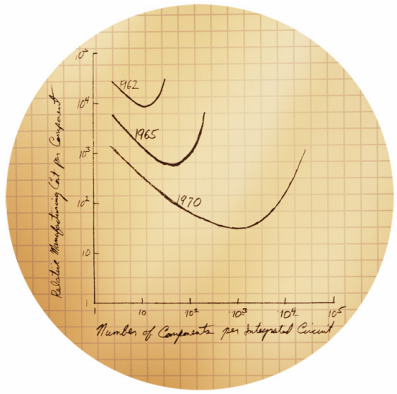

Figure 1 – G.E. Moore's original graph from 1965. Relative manufacturing cost per component versus number of components per integrated circuit [2]

Since the size of components in integrated circuits is shrinking in accordance with Moore's law, it is a simple matter to suggest that the ultimate integrated circuits will be constructed at the molecular or atomic level. Such a scenario was suggested in a 1959 lecture by the eminent physicist and visionary, Richard Feynman:

> *"I don't know how to do this on a small scale in a practical way, but I do know that computing machines are very large; they fill rooms. Why can't we make them very small, make them of little wires, little elements – and by little, I mean little. For instance, the wires should be 10 or 100 atoms in diameter, and the circuits should be a few thousand angstroms across...there is plenty of room to make them smaller. There is nothing that I can see in the physical laws that says the computer elements cannot be made enormously smaller than they are now. In fact, there may be certain advantages."* [3]

Speculation holds that silicon-based circuits will encounter a miniaturization limit, since at a point the quantum mechanical nature of electrons will dominate the behaviour of materials and alter the operation of future generations of electronic devices.

Molecular electronics can be defined as technology utilizing single molecules, small groups of molecules, carbon nanotubes, or nanoscale metallic or semiconductor wires to perform electronic functions. Potentially, this field provides a means to extend Moore's Law beyond the foreseen limit and that is why the concept of molecular electronics has aroused much excitement both in science fiction and among scientists. In this spirit, Aviram and Ratner proposed in 1974 a Gedanken experiment to realize a diode with a molecule connected at either end to metallic leads [4].

Recent progress in nanotechnology and nanoscience has facilitated both experimental and theoretical study of molecular electronics but an important issue to be settled is the accurate determination of the conductance of a single molecule. In

this paper different electronic transport measurement techniques are reviewed, in search of the most reliable ones in terms of the critical parameters that affect the measured properties during such experiments. A comparison of current per molecule values reported for alkane(di)thiols is also given.

2. Theoretical Background

2.1. Electron Transport in Molecules

Various electron transport (ET) mechanisms have been considered which depend on molecular size and structure, as well as on temperature. Electron transfer for the majority of systems can be described either by coherent nonresonant tunneling or coherent resonant tunneling. Coherent nonresonant tunneling occurs when the electronic states of the molecule are far from the energy of the tunneling electrons (e.g., transport in n-alkanethiols); the rate of electron transport is exponentially dependent on the length of the molecule. Coherent resonant tunneling occurs when the energy of the tunneling electrons is resonant with the energy of the molecular orbitals; the rate of electron transport is dominated by contact scattering, is essentially independent of length, and increases with the number of available modes [5].

In the next two sections these two main electron transport mechanisms will be briefly described. Complete discussions of more transport mechanisms such as hopping, Poole-Frankel effect, Fowler-Nordheim tunneling and Schottky emission are available in several reviews [6-8]. Table 1 lists these possible conduction mechanisms with their characteristic current, temperature, and voltage dependences.

Table 1 – Possible conduction mechanisms [9]

Conduction mechanism	Characteristic behavior	Temperature dependence	Voltage dependence
Direct tunneling	$J \sim V \exp\left(-\frac{2d}{\hbar}\sqrt{2m\Phi}\right)$	none	$J \sim V$
Fowler-Nordheim tunneling	$J \sim V^2 \exp\left(-\frac{4d\sqrt{2m}\Phi^{3/2}}{3q\hbar V}\right)$	none	$\ln\left(\frac{J}{V^2}\right) \sim \frac{1}{V}$
Thermionic emission	$J \sim T^2 \exp\left(-\frac{\Phi - q\sqrt{qV/4\pi\varepsilon d}}{kT}\right)$	$\ln\left(\frac{J}{T^2}\right) \sim \frac{1}{T}$	$\ln(J) \sim V^{1/2}$
Hopping conduction	$J \sim V \exp\left(-\frac{\Phi}{kT}\right)$	$\ln\left(\frac{J}{V}\right) \sim \frac{1}{T}$	$J \sim V$

2.1.1. Coherent Tunneling

Classical, or coherent, tunneling dictated by quantum mechanics is based on the probability of an electron traversing a barrier of some thickness and barrier height, and maintains the phase of the electron (Fig. 2). The rate of coherent tunneling decreases exponentially with the thickness of the barrier, and is given in its simplest form by the Simmons relation, eq. 1, where J =current density, q=electron charge, V=applied voltage, h=Plank's constant, m=electron mass, Φ=barrier height, and d=barrier thickness [10].

$$J = \frac{q^2 V}{h^2 d}\left(2m\Phi\right)^{\frac{1}{2}} \exp\left[-\frac{4\pi d}{h}\left(2m\Phi\right)^{\frac{1}{2}}\right] \quad (1)$$

Equation 1 shows only the linear term for a rectangular tunneling barrier, but it does show the exponential dependence on *d*. In the case of a molecular junction, *d* is the distance between conductors and Φ is the tunneling barrier height in joules or electron volts. Equation 1 is often simplified to a form useful for comparison to experiment, eq. 2, where *B* is a constant and β has units of inverse angstroms or inverse nanometers. By comparison to eq. 1, β is found to be proportional to the square root of the barrier height.

$$J = Be^{-\beta d} \quad (2)$$

Although observed tunneling rates in molecular junctions often depend exponentially on the junction thickness, the observed value of β is at times surprising. An observed β of 1.0 yields a barrier height of 0.96 eV according to the Simmons formula. This value is much smaller than the HOMO-LUMO gap of typical junction molecules (5-10 eV), so there must be more to the story than the Simmons model. A generally accepted explanation for faster than expected tunneling is "superexchange" [11-12]. Interactions of the electron with the orbitals and electronic structure of the molecule enhance the tunneling rate, making "through bond" tunneling more efficient than "through space" tunneling (see below). However, even a relatively small β of 0.5 $Å^{-1}$ predicts a decrease in the ET rate by a factor of >20000 for a 20 Å molecule, leading to the conclusion that coherent tunneling is effective only for short distances. Although tunneling, with or without superexchange, should not depend on temperature, the conformation of the molecule does. If molecular vibrations or internal rotations create a geometry with a smaller barrier to tunneling, the tunneling itself will appear to be temperature dependent [13]. Enhanced tunneling as a consequence of conformational changes is an example of an "activated" process which is expected to be temperature dependent. As a rule of thumb, coherent tunneling, even assisted by superexchange or conformational changes, is not effective over distances greater than ~25 Å, often less. ET over such distances is usually ascribed to more complex phenomena, such as "diffusive tunneling" or "hopping".

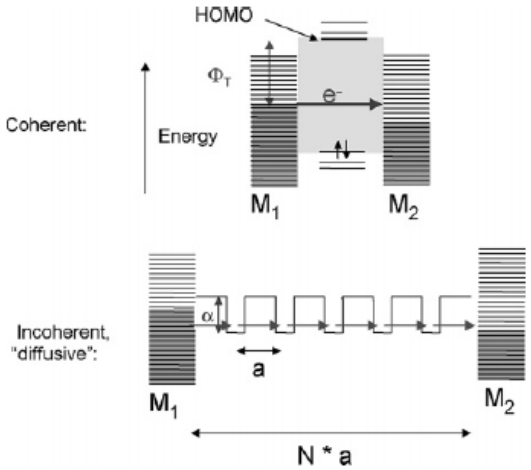

Figure 2 – Schematic energy level diagrams for coherent and diffusive tunneling. Φ_T is the barrier for coherent tunneling, R is the potential well depth of *N* sites spaced apart by a distance *a*. M1 and M2 are the metallic contacts [14]

2.1.2. Incoherent, Diffusive Tunneling

A surprising observation of the early 1990s was electron transport of an electron through ~40 Å of a DNA helix [15-16]. Since this distance was too large for coherent tunneling, and DNA was not known to be a "conductor" in the usual sense, another mechanism must be involved. Incoherent tunneling or the "tight binding" model proposes that the electron tunnels coherently along a series of sites, which are characterized by potential wells (Fig. 2) [17]. The residence time of the electron in a potential well is long enough to disturb the phase of the electron, and the process may be viewed as a series of discrete steps. It is "diffusive" because the path of the electron may follow a random walk between sites. However, it is important to recognize that the electron tunnels through the barriers between sites, and the process is not dependent on temperature to a first approximation.

2.2. Through Bond and Through Space Tunneling

It is generally assumed that the dominant current transport mechanism in molecular junctions is "through bond" (TB) tunneling, in which the current follows the bond overlaps along the molecule. However, there will always be a direct component from electrode to electrode, in which the molecule plays the role of a dielectric medium that modifies transport across the gap ("through space" (TS) tunneling). Figure 3 illustrates TB and TS tunneling for a molecular junction composed of tilted alkane chains.

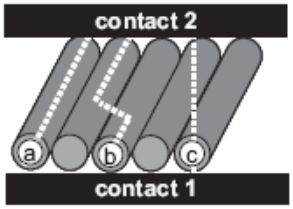

Figure 3 – Schematic illustration of (a,b) through bond (TS) and (c) through space (TS) tunneling in a molecular junction [18]

3. Electronic Transport Measurements

3.1. Single Molecules and SAMs

Some of the methods described in this section try to address single molecules, while in others several molecules (hundreds to thousands) are contacted. For most of the junctions considered, Self Assembled Monolayers (SAMs) of molecules are of great importance.

Self-assembly is a nowadays widely extended term that refers to the spontaneous formation of discrete nanometre-sized units, forming a secondary structure from simpler subunits or building blocks [19]. In the case of SAMs on solid surfaces, they can be easily formed by spontaneous adsorption from gas or liquid phases. Examples of SAMs on solid surfaces are thiols, silanes and phosphonates [20].

A specific covalent linker is used to guide the self-assembly process on each type of substrate. S or N atoms for clean metals and Si or P for hydroxilated surfaces and oxidized surfaces are some examples of usually employed linkers [20]. Among SAMs, the most popular because of both their promising and current applications in several fields of nanotechnology are alkanethiol (and alkanedithiol) monolayers on metals and metallic nanoparticles (particularly Au and Ag and, to a lesser extent, Cu, Ni, and Pd) [19]. Alkanethiols can also be self-assembled on semiconductor surfaces such as GaAs and Si oxide [21].

Each molecule in a SAM can be divided in three different parts: the head (linking group), the backbone (main chain), and the terminal specific (active) group (Fig. 4).

For alkanethiol SAMs on metal surfaces a sulfur atom links the hydrocarbon chain of variable length to the metal surface through a covalent bond. The van der Waals forces between neighbouring molecules stabilize the structure. Different angles define the orientation of the molecule with respect to the substrate.

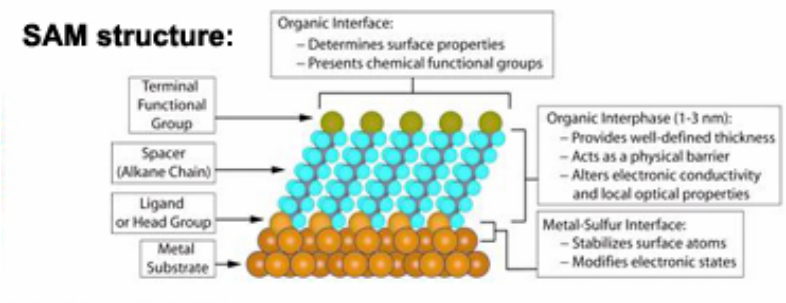

Figure 4 – SAM structure [22]

The alkyl chain ends in a terminal group and this confers the desired functional properties to the layer. A small change in the endgroup can be enough to change the physical and chemical properties of the layer [23, 24]. Thus, $–CH_3$ and $–CF_3$ groups turn the SAM surface hydrophobic, metallophobic and highly anti-adherent, while –COOH, $–NH_2$ or –OH groups yield hydrophilic surfaces with good metal ion and protein binding properties. Also, –SH-terminated thiols (termed dithiols) efficiently bind metallic ions and nanoparticles to the SAMs [19, 25].

3.2. Methods

A variety of experimental techniques have been developed to provide answers in questions such as the way electrons traverse a metal–molecule junction or how to macroscopically address a single to a few molecules. Many of these techniques can not only be used as a test-bed for measurements, but potentially be implemented in a usable device as well.

3.2.1. Contact Conductive Probe Atomic Force Microscopy (CP-AFM)

In CP-AFM, a metal-coated AFM tip is placed in direct contact with the SAM under a controlled load. The tip-SAM contact area is estimated to be about 15 nm^2, resulting in a junction of about 75 molecules [26].

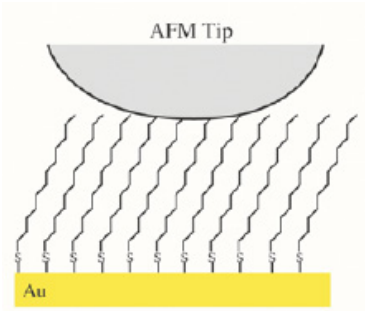

Figure 5 – An AFM tip in contact with a Self-Assembled Monolayer of alkanethiols [27]

Although this technique cannot measure the *I–V* characteristic across single molecules, it has the advantage that interpretation of the *I–V* curve is in some sense simplified because the probe is in direct and controllable contact with the SAM (force exerted on the sample by the tip). However, one should consider the effects of this tip-loading force on metal–SAMs–metal junction properties, since for different molecular structures different aspect of current-voltage characteristics is expected under this load [28]. Moreover, the exact number of molecules that interact with the tip, affecting the measured I-V characteristics, is debatable. Contact resistances of these junctions were also found to vary significantly based on the end group chemistry of the molecules, due to different partial charging at the SAM-tip interface [29].

3.2.2. Nanoparticle Coupled CP-AFM

Bifunctional (e.g. dithiol) molecules can be used to anchor Au nanoparticles to the surface by the formation of a covalent bond. In that way a metal–molecule–nanoparticle structure is formed, giving CP-AFM the potential for addressing single molecules (Fig. 6).

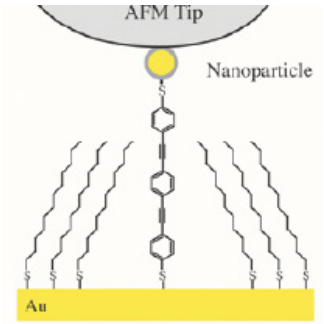

Figure 6 – Nanoparticle coupled CP-AFM [27]

Using directed assembly, isolated molecules with thiols on each end of the molecule can be inserted into insulating SAMs, leaving the terminal end of the molecule with a thiol exposed. The SAM is then exposed to gold nanoparticles allowing the terminal thiol to serve as an anchor that binds the nanoparticle to the surface. The most significant advantage of this technique is the ability to measure single molecules without a tunneling junction. Cui *et al.* found that when measuring dithiol SAMs, this junction produced larger currents (higher conductivity) and showed little to no variation with force [30]. In comparison, nonbonded contacts to octanethiol monolayers were at least four orders of magnitude more resistive, less reproducible,

and had a different voltage dependence, demonstrating that the measurement of intrinsic molecular properties requires chemically bonded contacts [31].

However, one complication is that the nanoparticle may be in contact with more than one molecule. When more than one molecule is in contact with the nanoparticle each molecule should independently and equally contribute to the measured current.

Another complication that needs to be taken into account is the role of the electronic effects of the nanoparticle (finite contact resistance with the AFM tip) [32].

3.2.3. Mercury Drop Junction

This approach, using a mercury drop as an electrode, is a relatively easy method to form a metal–molecule–metal junction. Similar to gold, mercury can form thiol-based SAMs. The junction is created by forming a mechanical contact of a SAM supported on a solid substrate and a SAM supported on a suspended mercury drop (Fig. 7). The resulting metal–SAM–SAM–metal junction allows for measurement of pure and mixed monolayers.

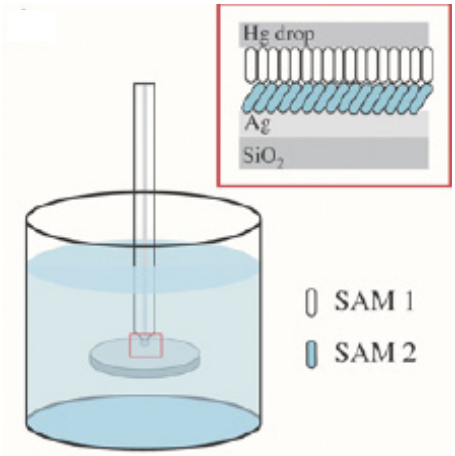

Figure 7 – Hanging Hg drop junction [27]

There are other variations of this system where both metal contacts can be Hg [33], or Hg–SAM–semiconductor structures can be formed [34]. These junctions are fast and easy to construct, allowing multiple SAM and metal combinations to be analyzed; however, this method is limited to ensemble measurements and cannot be performed at cryogenic temperatures [33]. In addition to that, these junctions require measurement of currents over significant areas (~1mm^2, or ~10^{12} molecules) of contact, and thus average variations in current due to boundaries between metal grains and organic domains, differences in local structure of the SAM, and defects [35]. Finally, such junctions cannot be developed into practically useful microelectronic components.

3.2.4. Scanning Tunneling Microscopy - Spectroscopy (STM - STS)

Use of a scanning probe microscope (SPM) allows the analysis of a few or even individual molecules. Much of the initial work done with scanning probes used STM (Fig. 8), where the topography is measured by monitoring a feedback loop that maintains a constant tunneling current. This technique has the advantage of being able to image and to measure the transport properties of individual molecules; however,

the interpretation of the *I–V* characteristics are complicated by the tunneling barrier inherent to the feedback mechanism of the STM tip, as the tunneling feedback forms a metal–molecule–gap-tip junction.

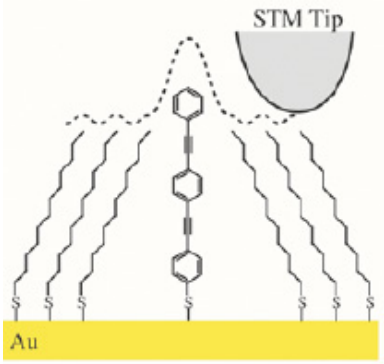

Figure 8 – Addressing a single molecule by STM [27]

Individual molecules can be isolated in an insulating SAM matrix and addressed by STM for characterization. As the inserted molecule is in a defect site, defining the exact environment of the molecule is quite difficult; therefore analytical measurements comparing different molecules cannot be made [36].

The STM tip acts as the second electrode, capable of imaging and addressing individual molecules but since topographic STM images are a convolution of the geometric and electronic structure of the tip and surface, it can be difficult to distinguish individual from bundled molecules.

3.2.5. Break junctions

3.2.5.1. Mechanically Controllable Break Junction

A mechanically controllable break (MCB) junction (Fig. 9) was one of the first techniques used to measure single-molecule conductance. This method uses a notched Au metal wire attached to a flexible substrate. The substrate is bent by a piezoelectric actuator until the notch fractures, producing a gap whose separation can be adjusted by the actuator, enabling an adjustable tunneling junction. After fracturing, a SAM of molecules from a solution is formed on each of the electrodes.

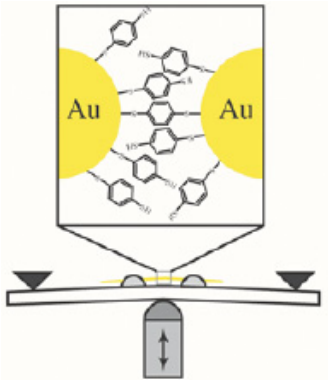

Figure 9 – A mechanically controllable break junction [27]

The electrodes are brought together until one molecule bridged both electrodes. While this system yields reproducible information on small and rigid molecules, it is not easily adapted for longer or more flexible molecules as the exact structure of the tunneling junction is unknown, and multiple contacts between other molecules in the junction could lead to the creation of unwanted parallel currents.

Indeed, theoretical interpretation of the data acquired from the benzene-1,4-dithiol system revealed that the origin of the observed properties could be the result of two molecules each bound to only one electrode where the overlap of the molecules provides electron transport if there is a high density of SAMs in the area of the junction or single-molecule conduction for dilute SAMs [37].

So several stable junctions with different *I–V* properties for the same molecule could be obtained and this emphasizes the difficulty of defining the environment and geometry of the molecules in this junction, making it difficult to fully understand the behaviour of the molecule in study.

3.2.5.2. STM Break Junction

Xu & Tao [38] developed an STM–break junction method that creates thousands of molecular junctions by repeatedly moving a scanning-tunneling-microscope tip into and out of contact with the substrate electrode in the presence of sample molecules (Fig. 10). The molecules in the study have two end groups that can bind to the tip and the substrate electrodes, respectively.

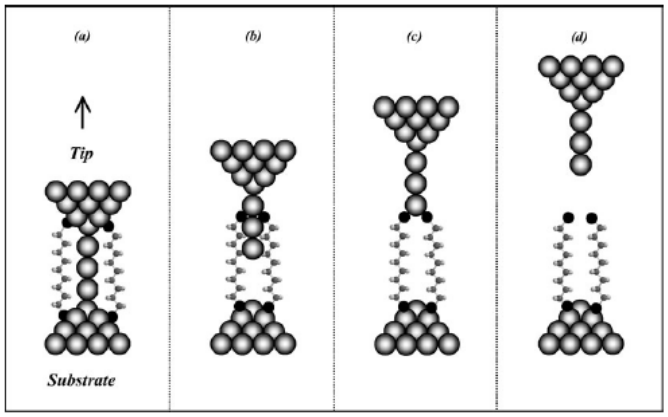

Figure 10 – A STM break junction. (a) initial formation of a gold atom chain (b) breakage of the atom chain, but conductivity is still maintained by short regions of the adsorbed molecules (c) molecular wires are formed (d) contact is broken [39]

The conductance histogram of these molecular junctions exhibits peaks located near integer multiples of a fundamental value, which is used as a signature to identify a single-molecule conductance [38]. This method selectively measures the conductance of those molecules bound to both electrodes.

The creation of the molecular junctions and the measurement of the conductance are performed in an organic solvent or aqueous electrolyte, so one can easily introduce the sample molecules via the solution and control the electron transport through the molecules electrochemically. At the same time though, one should consider the effects of the solvent on molecular transport [40].

Finally, the scanning-tunneling-microscope tip images the substrate surface before performing the electron-transport measurement, so one can place the tip on an

atomically flat area or move the tip laterally to a fresh area of the substrate during the measurement. This freedom however probably comes at the cost of mechanical and thermal stability.

3.2.5.3. Conducting AFM Break Junction

Xu and co-workers also measured the electromechanical properties of the molecular junctions with a conducting atomic force microscope (Fig. 11a) [32]. Each abrupt conductance decrease is accompanied by an abrupt decrease in the force, corresponding to the breakdown of a molecule from contacting the electrodes.

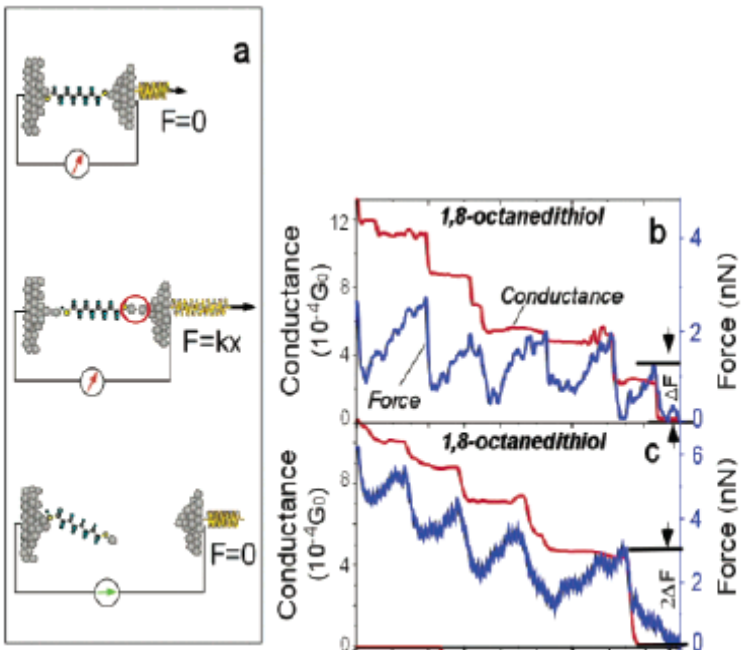

Figure 11 – (a) Schematic illustration of a molecule covalently bonded to two Au electrodes under mechanical stretching, during which both the conductance and the force are measured. (b-c) Simultaneously recorded conductance and force curves of octanedithiol junctions during stretching. (c) Shows that two molecules can break simultaneously at the last stage, resulting in twice as much change in the conductance and the force [41]

Further pulling causes only a slight change in the conductance but an approximately linear increase in the force. When the force reaches a certain threshold, another molecule junction breaks down, resulting in additional abrupt decreases in the conductance and the force. The conducting AFM break junction method allows one to study both the electronic and mechanical properties of single molecules.

What should be considered though for all break junction geometries, as already mentioned for CP-AFM, is how the straining effect on molecules during such measurements affects their properties.

3.2.6. Crossed Wire Junction

Crossed-wire tunnel junctions are formed by placing two wires, one of which is functionalized with a SAM, in a crossed geometry where one of the wires is perpendicular to an applied magnetic field (Fig.12). This junction, similar to the Hg

tunnel junctions, eliminates the difficulty associated with fabricating metal electrodes with extremely small gaps by having "mobile" electrodes.

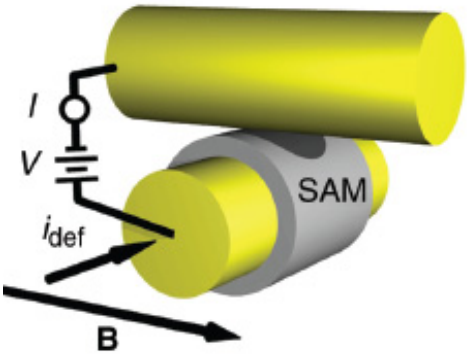

Figure 12 – Crossed wires [42]

The wire spacing is controlled by the Lorentz force (the deflection controlled by the DC current in the wire perpendicular to the magnetic field). This method has the advantage of forming a metal–molecule–metal contact without using an evaporated layer to form the second metal–molecule contact, decreasing the chance of damaging the organic layer, and increasing the ease of varying the identity of the metal contacts.

However, the number of molecules (chemically) contacted cannot be exactly specified and calculations based on comparison with other methods are used [43].

3.2.7. Nanowires

Cai and co-workers have developed a method to incorporate molecular junctions in metallic nanowires grown by template replication (Fig. 13) [44]

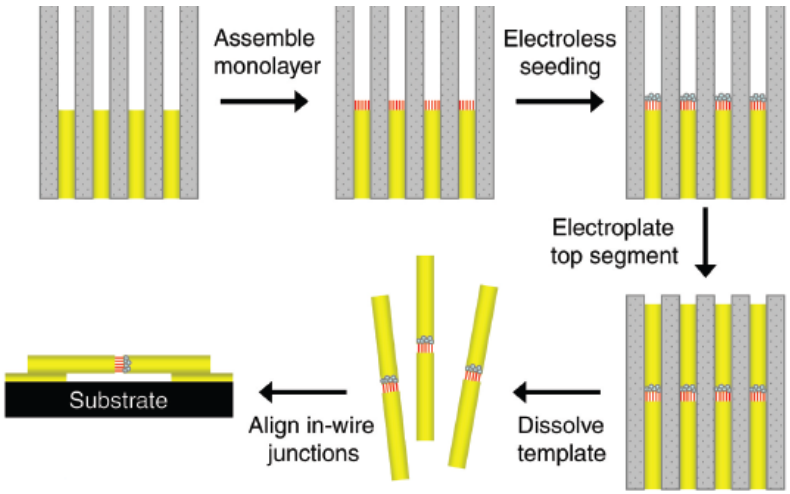

Figure 13 – In-wire junctions prepared by template replication [42]

Using template replication, metallic wires can be grown with nanometer-scale diameters but micrometers in length (Fig. 14). This provides a nanoscopic interface to the molecules while the microscopic length of the nanowire allows for connection to the outside world. One very different aspect of this configuration is that the top of the metal–molecule–metal junction is not evaporated, but rather uses a gentler electroless plating deposition.

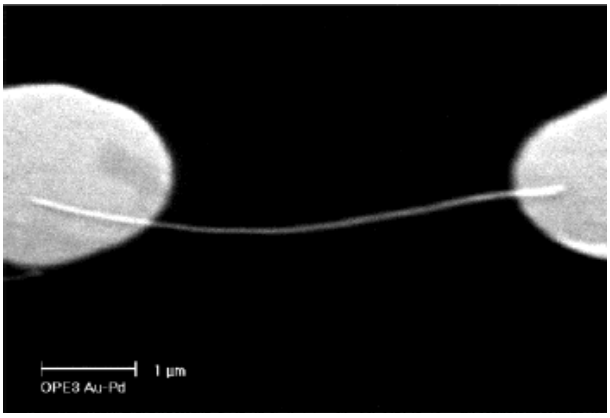

Figure 14 – Scanning Electron Microscopy image of a Au- oligo- (phenylene ethynylene) (OPE)-Pd nanowire contacted at each tip by a pair of Au pads **[44]**

The nanowires are can be aligned across two metallic contact pads using an AC electric field [45]. Once in contact, the metal–molecule–metal junction can be easily addressed.

One possible complication with this method involves the strain exerted on the SAM. As shown by CP-AFM, the force on the SAM can greatly influence the molecule's properties. It is possible that the SAM is under tensile or compressive strain in the nanowire, which could influence the behaviour of the system [28]. Also, it is difficult to know the structure or quality of the SAM during the formation of this junction and while mixed monolayers can be used in this system to decrease the number of active molecules being probed, this technique is used mostly for ensemble measurements.

3.2.8. Nanoparticle Bridge

A technique similar to the metal nanowires uses metallic nanoparticles to bridge the gap between two electrodes functionalized by candidate molecules (Fig. 15). The assembly is fabricated using a combination of photolithography and electron-beam lithography to grow Au electrode contacts with a gap of 40–100 nm. Using an AC electric field across the contacts a nanoparticle becomes trapped over the gap between the electrodes and closes the circuit. If a SAM is formed on the Au electrodes before the nanoparticle is trapped, a metal–molecule–nanoparticle– molecule–metal interface is formed [46].

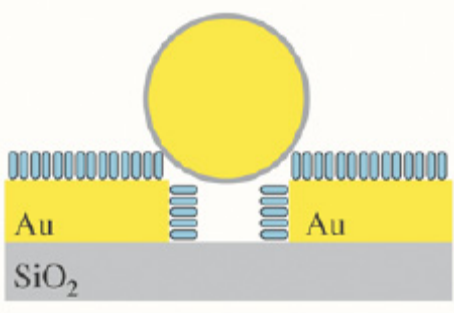

Figure 15 – A nanoparticle bridge **[27]**

A similar approach makes use of hemispherically metallized silica microspheres from the sequential deposition of Ni and Au layers. These microspheres are directed

magnetically onto SAM-functionalized electrodes to form molecular-based microsphere junctions (Fig. 16) [47].

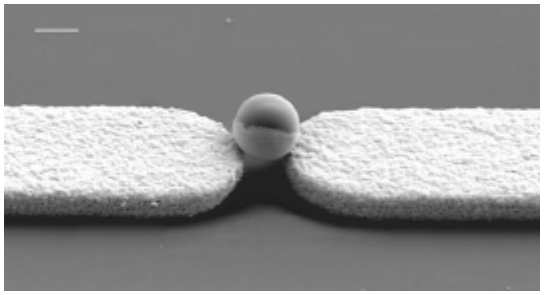

Figure 16 – A magnetically assembled microsphere junction [47]

This technique provides a unique method to demonstrate how these molecules may behave when connected in series. However, once again the number of molecules that contact the nanoparticle has to be estimated, based even on comparison with results previously reported by other methods [47].

Transport properties of alkanethiol molecules have also been estimated based on measurements on double-barrier tunneling structures formed with alkanethiol-protected Au nanoparticles (Fig. 17) [48].

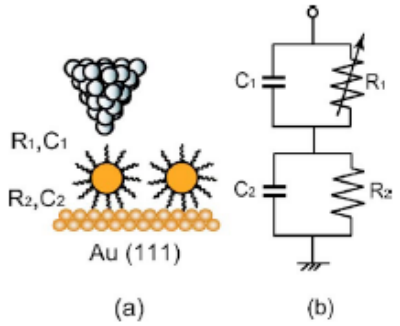

Figure 17 – (a) Schematic drawing and (b) equivalent circuit of the nanomechanical double-barrier tunneling structure [48]

3.2.9. Nanopores – Large-Area Diodes

Reed and co-workers have fabricated a structure, referred to as a nanopore (Fig. 18), to measure the conduction directly through a small number (thousands) of organic molecules [49].

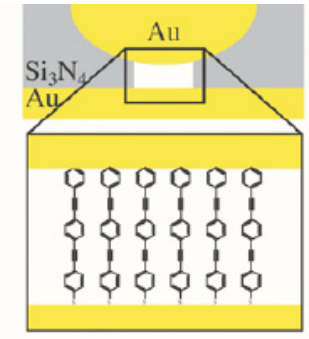

Figure 18 – A nanopore device [26]

The nanopore consists of a SAM of conjugated molecules sandwiched between two electrodes. The devices are fabricated using a combination of electron-beam lithography, plasma etching, and use of an anisotropic etchant to create a suspended silicon nitride membrane with a 30–50 nm aperture [49]. An Au contact is evaporated on the top of the aperture and the device is immersed in a solution of the molecule of interest to form a SAM. After deposition, the bottom electrode is formed by evaporating Au onto the sample, which is held at low temperature to minimize damage to the SAM; however, this deposition can still be quite harsh on the organic layer, damaging it and creating short-circuits between the two gold electrodes [50]. It is thus likely that the measured electrical characteristics represent an average of damaged as well as undamaged molecules. In an effort not to damage molecules noticeably, indirect electron beam evaporation of metals has been employed [51].

In any case, once the structure is sealed by the evaporated electrode, it is impossible to know the structure or status of the sandwiched organic layer. In addition, due to the geometry of the nanopore, it is not possible to determine the order or orientation of the SAM even before the top electrode is evaporated in place.

An elegant method to deal with the aforementioned problems with nanopores has been developed at the University of Groningen. This technique involves processing the molecular junctions in the holes of a lithographically patterned photoresist, and then inserting a conducting polymer interlayer between the SAM and the metal top electrode (Fig. 19) [52].

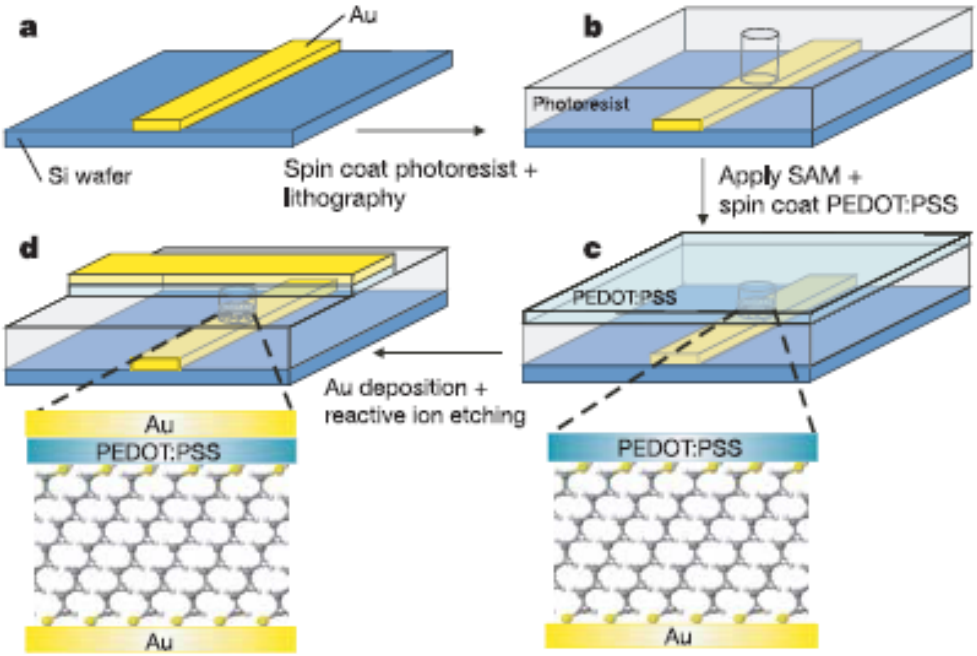

Figure 19 – Processing steps of a large-area molecular diode. (a) Gold electrodes are vapour-deposited on a silicon wafer and a photoresist is spin-coated. (b) Holes are photolithographically defined in the photoresist. (c) An alkanedithiol SAM is sandwiched between a gold bottom electrode and the highly conductive polymer PEDOT:PSS as a top electrode. (d) The junction is completed by vapour-deposition of gold through a shadow mask [52]

The use of the highly conducting polymer interlayer prevents short-circuits and the photoresist in which the structures are formed eliminates parasitic currents and

protects the junction from the environment. Results demonstrate that the polymer used (PEDOT:PSS) can be regarded as a non-interacting conductive electrode.

This method can be used to manufacture molecular junctions with diameters ranging from 10 to 100 μm with high yields (>95 %). The junctions show excellent stability and reproducibility. This simple approach is potentially low-cost and could pave the way for practical molecular electronics.

A critical parameter in this experiment is the quality (homogeneity in structure) of the SAM formed [53] over such a large area, since the density of the SAM molecules is needed for the current per molecule to be calculated.

3.2.10. Other Soft-Deposition Techniques

3.2.10.1. Nanotransfer Printing

Nanotransfer printing (nTP) has been introduced to fabricate top contact electrodes in Au/1,8-octanedithiol/GaAs junctions, in order to avoid direct Au/GaAs contacts (Fig. 20) [54]. In this experiment, conductive n^+ (001) GaAs (Si-doped, 10^{18} cm^{-3}) substrates rather than metallic bottom electrodes were chosen, because well-established models that describe electrical transport across metal-semiconductor interfaces could be used to evaluate the nature of contacts formed.

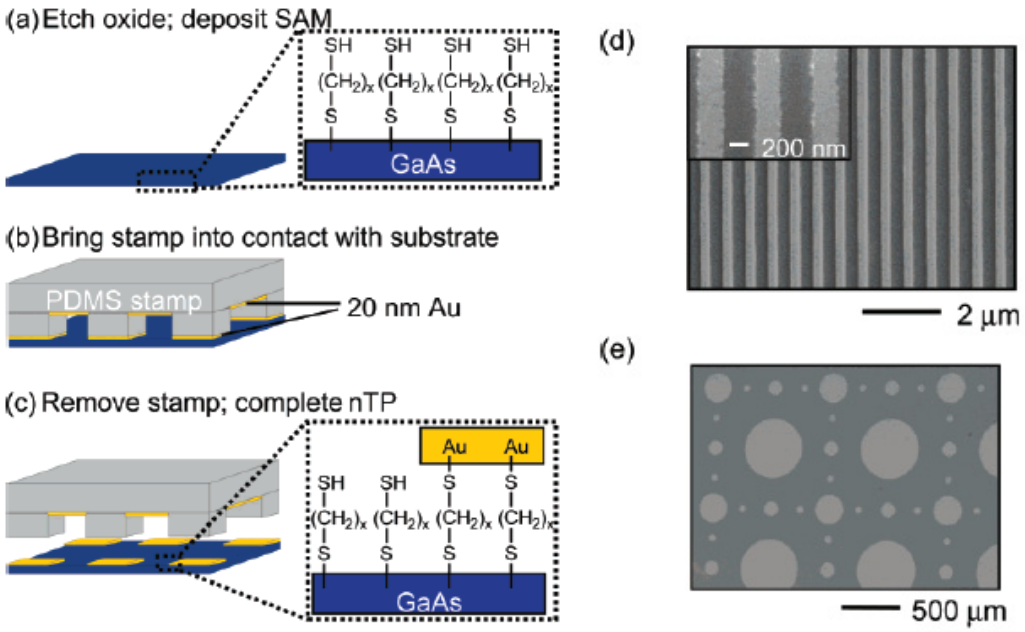

Figure 20 – Schematic of the nanotransfer printing (nTP) procedure. (a) The GaAs substrate is first etched and then exposed to 1,8-octanedithiol vapour (b) Gold-coated elastomeric PDMS stamp with appropriate relief features is brought into contact with the treated substrate (c) Removal of the stamp from the substrate completes the printing process. Scanning electron micrographs of (d) 300-nm-wide Au lines printed on an octanedithiol-coated GaAs surface and (e) nTP Au/dithiol/n+ GaAs junctions used in the transport studies [54]

Pattern transfer is purely additive (so the organic molecules are not subjected to etchants, sacrificial resists, or developers and solvents), and multiple devices can be fabricated in parallel. Nanotransfer printing is fast, simple, and occurs readily at ambient conditions.

3.2.10.2. Lift-Off/ Float-On (LOFO) and Polymer Assisted Lift-Off (PALO)

The term "lift-off" is taken from microelectronics, where it is used to describe the detaching of the photoresist layers, together with the evaporated metal on top of the resist. In the research of A. Vilan and D. Cahen it was used to describe the removal of a metal layer evaporated directly on a solid support [55]. The LOFO procedure consists of four major stages, namely:

1. Evaporation of the metal film onto a solid support.
2. Detaching the metal leaf from the solid support and floating it on a sub-phase liquid ("lift-off").
3. Adsorbing a molecular layer onto the target substrate, onto the metal leaf, or onto both, to add molecular functionality to the interface.
4. Attaching the metal leaf to the target substrate, in a liquid-mediated process (float-on).

The LOFO procedure is described schematically in Figure 21.

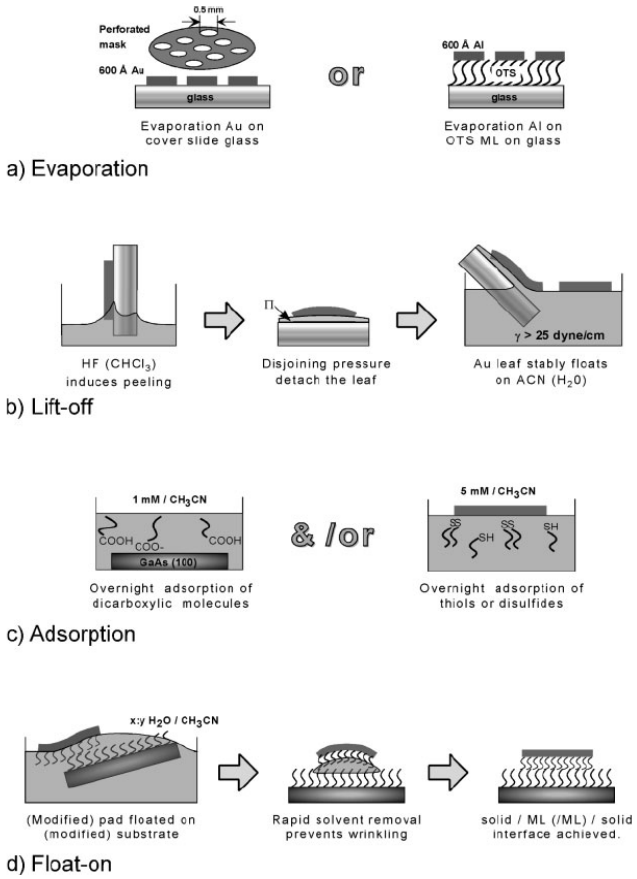

Figure 21 – Schematic description of the lift-off/ float-on procedure (LOFO) [55]

A similar, polymer-assisted lift-off (PALO), process has also been reported (Fig. 22) [56].

A drawback of the deposition of preformed electrodes is that attempts to create very large electrodes leads to wrinkled or torn metal films.

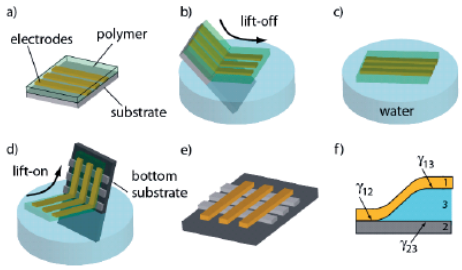

Figure 22 – Process for polymer-assisted, lift-off electrode deposition. (a) A hydrophobic backing layer is spin-cast onto metal electrodes patterned on a sacrificial substrate (b) After a brief etch, the metal–polymer layer cleanly lifts off onto the water surface upon immersion of the substrate (c) The polymer–metal film floats on the water surface without wrinkling owing to the surface tension of the water (d) A device is assembled by floating the metal–polymer film onto a bottom substrate, often patterned with electrodes and/ or molecular layers (e) A completed crossbar device (f) Definition of surface energies during metal–polymer deposition [56]

3.2.11. A Metal-Free Test Bed

A completely metal-free test bed has been developed, that eliminates the possibility of metal nanofilament formation and ensures that molecular effects are measured. This system uses single-crystal silicon and single-walled carbon nanotubes as electrodes for the molecular monolayer [57]. The fabrication procedure for this testbed is shown in Figure 23.

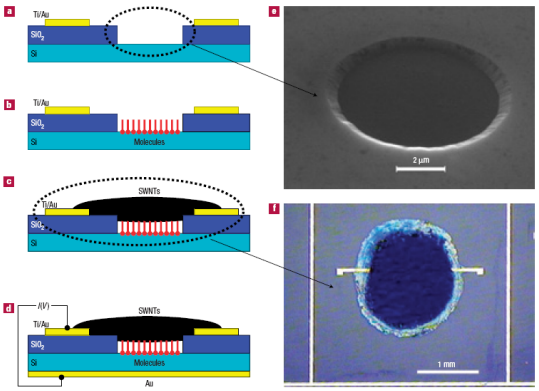

Figure 23 – A schematic of the Si–molecule–SWNT device and its fabrication process. (a)The starting lithographically defined structure (b) Formation of a molecular monolayer in the well (c) Deposition of a SWNT mat on top of the molecules and across the well, electrically connecting the molecular layer to the metal pads (d) Finished device, after bottom-side Au contact formation (e) A scanning-electron-microscope image of a 5-μm well showing its ramped oxide edges (f) The top view of a finished device [57]

However, the special conduction features of carbon nanotubes (i.e. dependence on chirality) make the determination of their effect on the measured transport properties rather difficult.

3.3. Results of Transport Measurements of Alkane(di)thiols

Reported results of electronic transport measurements on alkanethiol and alkanedithiol molecules by several of the aforementioned techniques are given in Table 2.

Table 2

	Junction[a]	Decay Coefficient β [Å^{-1}] [b]	Resistance per molecule (bias voltage)[c]	Current per molecule at 0.2V bias[d]	Method	Reference
1	Au-S-C6/Au	0.79	-	80pA	Nanoparticle Bridge	[58]
2	Au-S-C6-S-Au	0.92	10.5 MΩ (<0.3V)	20000pA	STM Break Junction	[38]
3	Au-S-C6-S-Au	0.77	-	50pA	STM Break Junction (in solution)	[59]
4	Au-S-C6-S-Au	0.84	15MΩ (0.1V)	14000pA	STM-AFM Break Junction	[60]
5	Au-S-C8/Au	0.83	-	14pA	Nanopore	[61]
6	Au-S-C8/Au	0.75	-	0.015pA	CP-AFM (in solution)(6nN)[e]	[30]
7	Ag-S-**C8-C16**-S-Hg	0.87	-	0.008aA	Mercury Drop	[35]
8	Au-S-C8-S-Au	-	900MΩ (0.1V)	220pA	Nanoparticle Coupled CP-AFM (in solution)(6nN)[e]	[31]
9	GaAs-S-C8-S-Au	-	-	0.00004aA	Nanotransfer Printing	[54]
10	Au-S-C8-S-Au	-	-	20pA	Nanopore	[62]
11	Au-S-C8-S-PEDOT:PSS-Au	0.66	-	0.2pA	Large Area Diode	[52]
12	Au-S-C8-S-Au	0.52	1000MΩ (0.5V)	200pA	STM Break Junction	[39]
13	Au-S-C8-S-Au	-	300MΩ (0.2V)	700pA	Mechanically Controllable Break Junction (in solution)	[63]
14	Au-S-C8-S-Au	0.84	50MΩ (0.1V)	4000pA	STM-AFM Break Junction	[60]
15	Au-S-C8-S-Au	0.77	-	22pA	STM Break Junction (in solution)	[59]
16	Au-S-C12/Au	0.83	-	0.17pA	Nanopore	[61]
17				0.2-0.02pA	CP-AFM (5-20nN)[e]	
18	Au-S-C12/Au	0.98	-	0.03pA	CP-AFM (10nN)[e]	[28]
19	Au-S-C12/Au	0.79	-	0.25pA	Nanoparticle Bridge	[58]
20	Hg-S-C12/p-Si	0.55	-	0.6pA	Mercury Drop	[64]
21	Au-S-C12-S-PEDOT:PSS-Au	0.66	-	0.008pA	Large Area Diode	[52]
22	Au-S-C12-S-Pd	-	200GΩ	1pA	Nanowire	[44]
23	Au-S-C12-S-Au	-	-	10pA	Crossed Wires	[43]

[a] Cn stands for $(CH_2)_n$ in case of dithiols and $(CH_2)_{n-1}CH_3$ for thiols [b] some values were calculated from reported β/methylene values [c] some values calculated from conductance values [d] some values calculated from current densities assuming the area of an alkane(di)thiol molecule to be 0.217nm^2 [52], or calculated assuming ohmic (linear) behavior in low biases [e] value in parentheses is the tip load force

The dispersion of values summarized in Table 2 proves and presents quantitatively the points considered for each measurement technique in the previous section. Taking the octane(di)thiol molecule for example, a graph of reported current per molecule versus the area of the contact can be drawn. This is given in Fig. 24.

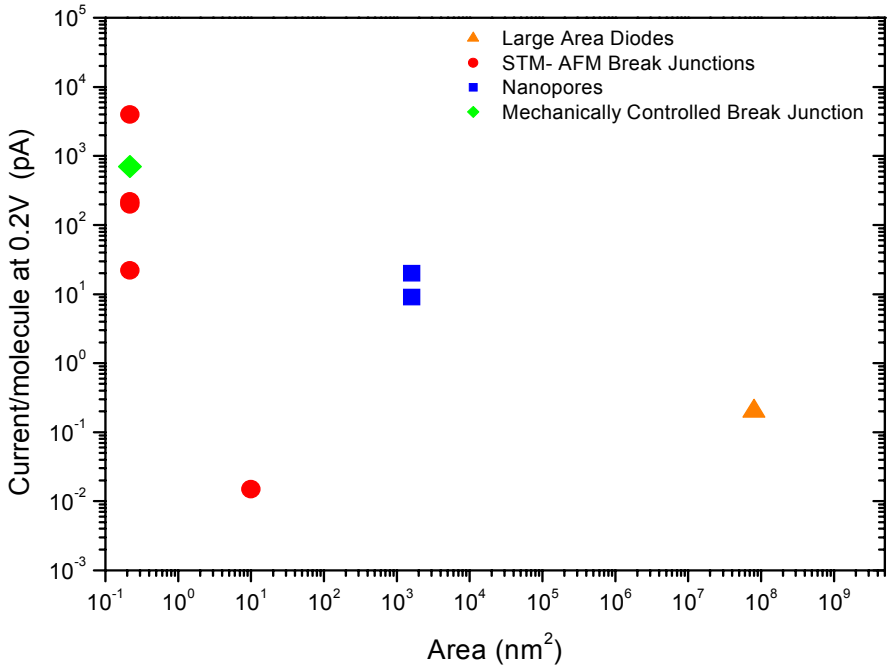

Figure 24 – Graph of current per molecule versus device area. Currents from Table 2 and junction areas from [30, 52, 61, 62]. When single molecules were addressed the value 0.217nm² [52] is used for the junction area.

It is noteworthy that currents/molecule measured by STM-AFM break junction geometries differ up to 5 orders of magnitude. Nanopores and large-area junctions, which have similar device geometries, still differ by ~2 orders of magnitude (more than the alleged difference [52]).

Possible reasons for these variations are considered in the following section.

4. The critical Parameters

In many of the experimental techniques reviewed, a difficulty in estimating the number of molecules in the junction exists. Though, even if small differences in reported currents/molecule might be explained on the basis of this uncertainty, it is unlikely that such factors alone can account for the large discrepancies seen in Table 2. Other factors, such as the properties of electrodes, contact geometry, and effects of local environment need to be considered.

4.1. Electrodes

It is clear that the measured conductance, apart from the molecule itself, depends also on the properties of the electrodes. Firstly, the alignment of the molecular energy levels, especially the highest occupied molecular orbital (HOMO) and lowest

occupied molecular orbital (LUMO), relative to the Fermi levels of the electrodes affect conductance. This energy-level alignment is determined by the intrinsic properties of the molecule and the electrodes, and also by the interactions between them, which are often difficult to determine for both theory and experiment [65, 66]. Changing the metal used for the fabrication of the electrodes alters the characteristics of the contact [67]. Secondly, in case of SAMs (additional) defects and shorts can be introduced during the fabrication of the top electrode and ways to avoid these problems have already been mentioned (indirect or in vacuum evaporation, application of a protective layer of conductive polymer before evaporation and nanotransfer printing). Thirdly, even though the molecules have two linker groups (alkanedithiols), it is difficult to determine if the molecules are indeed covalently bound to the both electrodes. The presence of physical contacts introduces an additional barrier in the junction.

The effects of these three points can be seen in the differences between entries 5, 9 and 11 of Table 2. The extremely low current observed by the nanotransfer printing technique shows that the covalent linking of the 1,8-octanedithiol molecules to the "printed" top gold electrode is in all probability not efficient enough. The different interfaces (molecule/semiconductor, molecule/metal) might also contribute to the observed variations.

4.2. Contact Geometry

In the scanning probe microscopy methods (STM and AFM) the tip molecule contact is not as well-defined as the molecule-substrate contact. The conductance measured when a single-molecule junctions is formed has been found to vary considerably from one junction to another, indicating variations of the contact geometries [68]. Figure 25 shows various configurations of an 1,6-hexanedithiol molecule between two electrodes and the calculated respective conductances.

Such conformational differences have been used by Li and co-workers to explain the high and low values for conductance found during their studies of alkanedithiol molecules with the STM break junction setup [60].

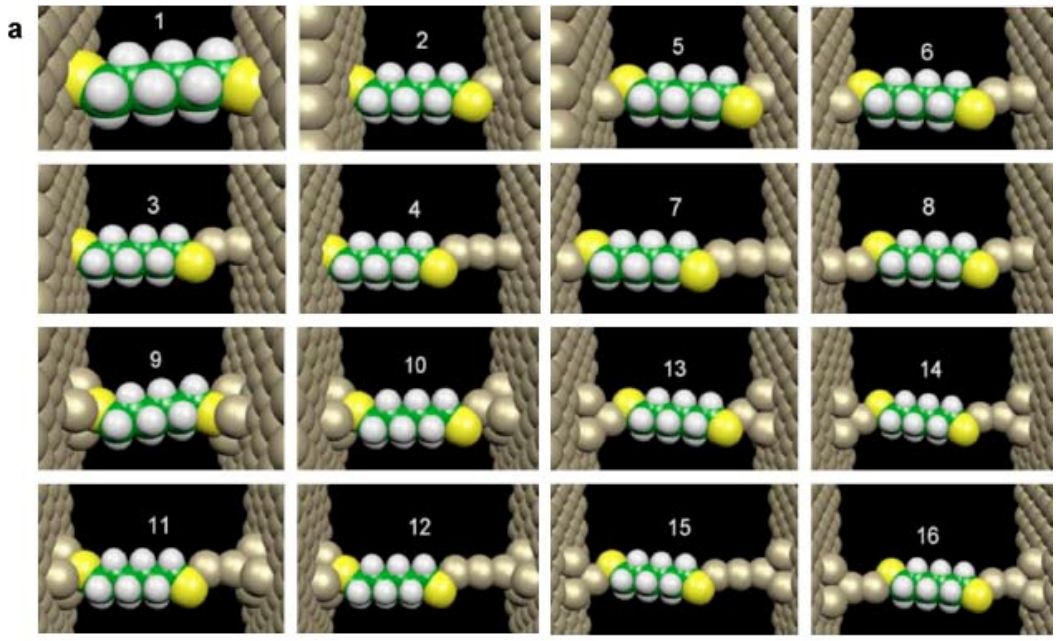

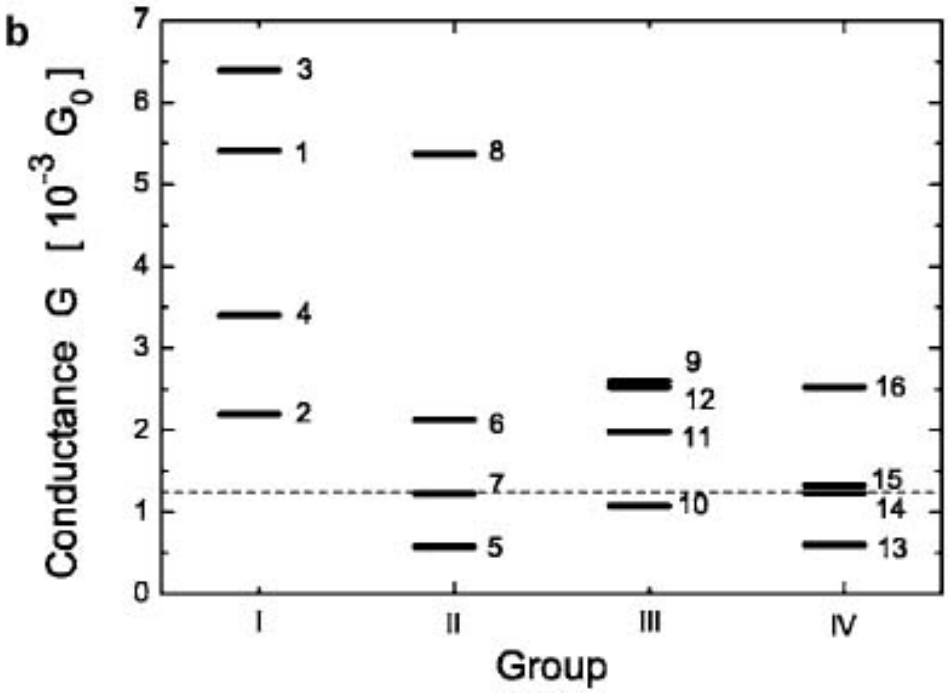

Figure 25 – (a) Different contact geometries of a 1,6-hexanedithiol molecule bound to two Au electrodes. (*b*) Calculated electrical conductance values of a single 1,6- hexanedithiol molecule for the different electrode configurations 1–16. The dashed line indicates the experimental conductance value found by Xu and Tao **[38]**. *G*0 is the quantum conductance **[68]**

The varying, by a factor of 6, results of the group of Wang on the specific STM break junction geometry [9, 61, 62] emphasizes the difficulty to construct well-defined contacts.

4.3. Local environment

Another factor that may affect the measured conductance is the local environment of the molecule, which includes solvent molecules (vacuum or air [40]). As seen from entries 6 and 8 of Table 2, solvent effects can become important in case of non-covalent bonding. The current observed for the 1-octanethiol, that is physically contacting the gold AFM tip, is several orders of magnitude lower that that of the 1,8-octanedithiol that is chemically bonded to both gold substrate and nanoparticle. That can be attributed to a solvation shell around the tip that reduces the electronic coupling to the molecules [18].

Another way in which the environment can affect the conductance of a molecule is through energy exchange of the traversing electron with the vibrational modes of the solvent molecules [69].

The studies of Selzer and co-workers also show that the normalized coherent conduction at low applied bias and low temperature is essentially the same for both single-molecule and SAM junction configurations. In contrast, the conduction through an individual isolated molecule increases rapidly with increasing bias and becomes comparable to the conductance of several thousand otherwise identical molecules packed in a self-assembled monolayer. These results underscore the practical importance of correlating local environment with electrical properties when designing molecular electronic devices [70].

4.4. Local Heating

Local heating is a well-known critical parameter in the design of conventional silicon-based microelectronics. As far as single molecules are concerned, an important question is how hot they get when current passes through them. In such a nanoscale junction, the inelastic electron mean free path is often large compared with the size of the junction, so each electron is expected to release only a small amount of its energy to phonons (heat) during transport in the junction [18,71]. However, substantial local heating may still arise owing to the large current density and thus power per atom. For example, in octanedithiol, the temperature with a bias voltage of 1 V (current ~20nA) was found to increase by ~25 K above room temperature [72].

4.5. Forces

In the case of mechanical methods such as break junctions, a question on how the applied force affects the measured conductance of the molecules arises. One can expect that the molecular chain is compressed making tunneling distance shorter, or tilted resulting in increased chain-to-chain coupling when the tip-loads are applied to molecular layers.

What was measured by AFM though was that the breakdown force of a molecular junction is ~1.5nN and occurs at the Au-Au bond [60]. Thus, that is the maximum force that one can to the molecule bonded between the two gold electrodes. For molecules such as alkanedithiols, such a force is of course not sufficient to change the electronic states of the molecules or distort the structure of the molecule significantly. Contrary to that, for flexible conjugated molecules such as oligothiophenes the force can cause a much greater change in the conductance.

However significant changes in conductance have been reported even for alkanedithiols at large tip loads [28].

5. Conclusions

The field of molecular electronics has advanced significantly ever since it's appearance in the 1970's. The theory of molecular transport has evolved to a point where basic conduction through organic molecules is fairly understood. But the bottleneck of molecular electronics research remains in the area of characterization. Developing reliable, reproducible and well-understood characterization testbeds is essential for the further understanding of molecular transport.

Effects such as the electrostatic potential distribution across the molecular bridges, local heat conduction, coupling to the contacts and electron-vibrational mode coupling render a comprehensive analysis of molecular transport rather complicated. Thus, local molecular environment can have a profound influence on molecular conduction.

As a result, electrical measurements in devices with large molecular ensembles are not for the moment directly comparable with single-molecule conductance measurements, since this inevitably relies on normalization to a single molecule. A solid understanding and theoretical analysis of the parameters that affect and govern electron transport through molecules will eventually allow such quantitative comparisons and make the results of the two approaches converge.

Until then, based on the fact that the widest variations of the aforementioned effects can be expected for the cases of junctions containing a single isolated molecule or an individual molecule embedded in a densely packed monolayer, the author's belief is that well-defined structures incorporating self assembled monolayers like nanopores and wide-area diodes shall be providing the most reliable results.

These techniques can possibly be used to materialize molecular electronic devices that might be challenging silicon technology in a few years and why not replace it at the end of its roadmap.

6. Acknowledgements

I would like to thank Dr. Bert de Boer for assigning and supervising the writing of this paper. I would also like to express my gratitude to Markella, for kindly allowing me to work, while she wandered alone through the beauties of Groningen. Finally, I would like to acknowledge the financial support of the Public Welfare Foundation "Propondis", that offers me the chance to study abroad without having to encumber my family.

7. References

[1] Moore, G.E. *Electronics* 1965, 38, 8.
[2] http://www.intel.com/pressroom/kits/events/moores_law_40th/index.htm
[3] Richard Feynman gave this talk entitled "There's Plenty of Room at the Bottom" on December 29th, 1959, at the annual meeting of the American Physical Society at the California Institute of Technology.
[4] Aviram, A.; Ratner, M. A. *Chem. Phys. Lett.* 1974, 29, 277.
[5] Weiss P.S.; Bumm L.A.; Dunbar T.D.; Burgin T.P.; Tour J.M.; Allara D.L. *Molecular Electronics: Science and Technology* 1998, 852, 145–168.
[6] Heath, J. R.; Ratner, M. A. *Phys. Today* 2003, 56, 43.
[7] Joachim, C.; Gimzewski, J. K.; Aviram, A. *Nature* 2000, *408*, 541.
[8] Schwab, P. F. H.; Levin, M. D.; Michl, J. *Chem. Rev.* 1999, *99*, 1863.
[9] Wang, W. et al. *Phys. Review B* 2003, 68, 035416.
[10] Simmons, J. G. *DC Conduction in Thin Films*; Mills and Boon Ltd.: London, 1971.
[11] Abu-Hilu, M.; Peskin, U. *Chem. Phys.* 2004, *296*, 231.
[12] Newton, M. D. *Theor. Chem. Acc.* 2003, *110*, 307.
[13] Selzer, Y.; Cabassi, M. A.; Mayer, T. S.; Allara, D. L. *J. Am. Chem. Soc.* 2004, *126*, 4052.
[14] McCreery, R. L. *Chem. Mater.* 2004, 16, 4477-4496
[15] Murphy, C. J. et al. *Science* 1993, *262*, 1025.
[16] O'Neill, M. A.; Dohno, C.; Barton, J. K. *J. Am. Chem. Soc.* 2004, *126*, 1316.
[17] Mujica, V.; Roitberg, A. E.; Ratner, M. A. *J. Phys. Chem.* 2000, *112*, 6834.
[18] Salomon A. et al. *Adv. Mater.* 2003, 15, 1881.
[19] Love, J.C. et al. *Chem. Rev.* 2005, 105, 1103.
[20] Schreiber, F. *J. Phys.: Condens. Matter* 2004, 16, R881.
[21] Pavlovic, E. Et al. *Nano Lett.* 2003, 3**,** 779.
[22] http://gmwgroup.harvard.edu/research_surfacescience/figure1_big.jpg
[23] Ulman, A. *Chem. Rev.* 1996, 96, 1533.
[24] Pflaum, J. et al. *Surf. Sci.* 2002, 498, 89.
[25] Gittins, D.I. et al. *Nature* 2000, 408, 67.
[26] Wold, D.J.; Frisbie, C.D. *J. Am. Chem. Soc.* 2001**,** *123,* 5549
[27] Mantooth, B.A.; Weiss, P.S. *Proceedings of the IEEE*. 2003, 91, 1785.
[28] Song, H et al. *Colloids and Surfaces A: Physicochem. Eng. Aspects* 2006, 284–285, 583.
[29] Gosvami, N. et al. *Applied Surface Science* 2006, 252, 3956.
[30] Cui, X.D. et al. *Nanotechnology* 2002, 13,5.
[31] Cui, X.D. et al. *Science* 2001, 294, 571
[32] Tomfohr, J. et al. *Lecture Notes In Physics* 2005, 680,301.
[33] Rampi, M.A.; Whitesides, G.M. *Chem. Phys.* 2002, 281, 373.
[34] Selzer, Y.; Salomon, A.; Cahen, D. *J. Amer. Chem. Soc*. 2002, 124, 2886.
[35] Holmlin, R.E. et al. *J. Am. Chem. Soc.* 2001**,** *123,* 5075.
[36] Bumm, L. A. et al, *J. Phys. Chem. B* 1999, 103, 8122.
[37] Emberly, E.G.; Kirczenow, G. *Phys. Rev. B* 2001, 64, 235412.
[38] Xu, B.; Tao, N.J. *Science* 2003, 301, 1221.
[39] Haiss, G. et al. *Phys . Chem. Chem. Phys*. 2004, 6, 4330.
[40] Long, D.P. et al, *Nature Materials* 2006, 5, 901.
[41] Xu, B.; Xiao, X.; Tao, N.J. *J. Am. Chem. Soc.* 2003, 125, 16164.
[42] Kushmerick, J.G. et al, *MRS Bulletin,* June 2004
[43] Kushmerick, J.G. et al, *J. Am. Chem. Soc.* 2002, 124, 10654.

[44] Cai, L.T. et al. *J. Phys. Chem. B* 2004, *108,* 2827.
[45] Smith, P.A. et al. *Appl. Phys. Lett.* 2000, 77, 1399.
[46] Amlani, I. et al. *Appl. Phys. Lett.* 2002, 80, 2761.
[47] Zhang, H. et al. *Physical Review B* 2005, 72, 205441.
[48] Long, D.P. et al. *Appl. Phys. Lett*. 2005, 86, 153105.
[49] Zhou, C. et al. *Appl. Phys. Lett.* 1997, 71, 611.
[50] de Boer, B. et al. *Langmuir* 2004**,** *20,* 1539.
[51] Haick, H. et al. *Phys . Chem. Chem. Phys* . 2004, 6, 4538.
[52] Akkerman, H.B.; Blom, P.W.M.; de Leeuw, D.M.; de Boer, B. *Nature* 2006, 441,69.
[53] Vericat, C. et al. *J. Phys.: Condens. Matter* 2006, 18, R867
[54] Yueh-Lin Loo et al. *Nano Letters* 2003, 3, 913.
[55] Vilan, A.; Cahen, D. *Adv. Funct. Mater*. 2002, 12, 795.
[56] Shimizu, K.T. et al. *Adv. Mat.* 2006, 00,1.
[57] Jianli, H. et al. *Nature Materials (Advance Online Publication)* 2005, 1.
[58] Chu, C. et al. *J. Am. Chem. Soc.* 2007, 129, 2287.
[59] Wierzbinski, E.; Slowinski, K. *Langmuir* 2006*,* 22, 5205.
[60] Li, X. et al. *J. Am. Chem. Soc.* 2006, 128, 2135.
[61] Lee, T. et al. *Current Applied Physics* 2005, 5, 213.
[62] Wang, W. et al. *Nano Letters* 2004, 4, 643.
[63] Gonzalez, M.T. et al. *Nano Letters* 2006, 6, 2238.
[64] Selzer, Y. et al. *J. Phys. Chem. B* 2002, 106, 10432.
[65] Xue, Y. et al. *J. Chem. Phys*. 2001, 115, 4292.
[66] Heimel, G. et al. *Phys. Rev. Lett*. 2006, 96, 196806.
[67] Beebe, J. M. et al. *J. Am. Chem. Soc.* 2002, 124, 11269.
[68] Muller, K.H. *Phys. Rev. B* 2006, 73, 045403.
[69] Nitzan A. *Annu. Rev. Phys. Chem*. 2001,52, 681.
[70] Selzer, Y. et al. *Nano Letters* 2005, 5, 61.
[71] Wang, W. et al. *J. Phys. Chem. B*. 2004, 108, 18398.
[72] Huang, Z.F. et al. *Nano Letters* 2006, 6, 1240.